Yukon

MR-23-02

Predictive Wetland Mapping

Mayo and McQuesten Watersheds, Yukon

September 2023

Predictive Wetland Mapping: Mayo and McQuesten Watersheds, Yukon

Government of Yukon
Fish and Wildlife Branch
MR-23-02

Author[s]
WSP E&I Canada Limited

Copies available from:
Environment Yukon
Fish and Wildlife Branch, V-5
Box 2703, Whitehorse, Yukon Y1A 2C6
Phone (867) 667-5721
Email: environmentyukon@gov.yk.ca
Online: www.env.gov.yk.ca

Suggested citation:
WSP E&I CANADA LIMITED. 2023. Predictive Wetland Mapping: Mayo and McQuesten Watersheds, Yukon (MR-23-02). Government of Yukon, Whitehorse, Yukon, Canada.

PREDICTIVE WETLAND MAPPING

MAYO AND MCQUESTEN WATERSHEDS, YUKON

GOVERNMENT OF YUKON

PROJECT NO.: CE05106
DATE: MARCH 2023

WSP E&I Canada Limited
5681 70 Street NW
Edmonton, AB T6B 3P6

T: +1 780-436-2152

WSP.com

31 March 2023

Nadele Flynn
Fish and Wildlife, Environment
Government of Yukon
10 Burns Road
Whitehorse, Yukon Y1A 4Y9

Dear Ms. Flynn:

Subject: Wetland Mapping, Mayo and McQuesten Watersheds, Yukon

This report has been prepared for the Government of Yukon, with specific application to the Mayo and McQuesten Watersheds, Yukon Predictive Wetland Mapping Project. This report and its accompanying map for wetlands found in the study area is based on the field survey data collected in 2021.

Any use which a third party makes of this report, or any reliance on or decisions made based on it, are the responsibility of such third parties. WSP E&I Canada Limited (WSP) accepts no responsibility for damages, if any, suffered by any third party because of decisions made or actions based on this report. The work was conducted in accordance with the scope of work prepared for the Project, and generally accepted remote sensing and biological work practices. No other warranty, expressed or implied, is made.

Should you have any questions, please contact the undersigned at your earliest convenience.

Yours sincerely,

Rebecca Warren, M.Sc.
Remote Sensing and GIS Specialist

RW/cj

WSP E&I Canada Limited
5681 70 Street NW
Edmonton, AB T6B 3P6

T: +1 780-436-2152
wsp.com

QUALITY MANAGEMENT

ISSUE/REVISION	FIRST ISSUE	REVISION 1	REVISION 2	REVISION 3
Remarks		Updated to reflect report revisions requested by Government of Yukon	Updated to address edits/comments requested by Government of Yukon	
Date	31 March 2022	20 March 2023	30 March 2023	
Prepared by	Rebecca Warren	Rebecca Warren	Rebecca Warren	
Signature				
Checked by	Meisam Amani	Meisam Amani Deo A Heeraman	Deo A Heeraman	
Signature				
Authorized by	Deo A Heeraman	Deo A Heeraman	Deo A Heeraman	
Signature				
Project number	CE05007	CE05106	CE05106	
Report number				
File reference				

EXECUTIVE SUMMARY

This report accompanies and discusses the mapping of wetland areas and adjacent non-wetland areas in the Mayo and McQuesten watersheds, including five areas of special interest, developed by WSP E&I Canada Limited (WSP) under contract with Government of Yukon. Wetland areas were classified according to the Canadian Wetland Classification System and include shallow water (less than 2 m deep), bogs, fens, marshes, and swamps. Non-wetland areas were identified as deep water (greater than 2 m deep), exposed/disturbed, forested/shrub, and grassland. Wetlands were classified using an object-based Random Forest model in eCognition (version 10.1) using optical (i.e., Sentinel-2) and Synthetic Aperture Radar (i.e., Sentinel-1, ALOS PALSAR) satellite imagery, and topographic data (i.e., merged Canadian Digital Elevation Model and ArcticDEM). Model training and assessment data was acquired through both field surveys and the interpretation of high-resolution satellite imagery (i.e., drone, SPOT 6/7, and Esri World Basemap Imagery). Field surveys were conducted by Government of Yukon and WSP in July and August 2021, and included information on site dominant vegetation, soil characteristics, landscape position, and preliminary ecosite association. Interpreted sites were assigned one of the five wetland or four non-wetland classes only. A polygon was manually delineated for each field and interpreted site and used as inputs for the segmentation and split 50/50 for training and assessing the Random Forest model. The classification was manually refined to correct errors, such as shadows in the input imagery being mapped as water, by changing an object's mapped class or altering object boundaries. The final classification was assessed visually and statistically for accuracy by Government of Yukon, WSP and First Nation of Na-Cho Nyak Dun. Based on the results, approximately 7% of the total area within the Mayo and McQuesten watersheds is comprised of wetlands, with a coverage of only approximately 5% of the areas of interest. The overall wetland classification accuracy was 98.66% (Kappa coefficient equals 0.98) for wetland versus and non-wetland classes and 88.32% (Kappa coefficient equals 0.82) for the five wetland classes. These results show that the approach used in this project offers great potential for wetland classification in future studies and will assist in management decisions related to land use planning and management of the Mayo and McQuesten watersheds.

TABLE OF CONTENTS

TABLES

FIGURES

APPENDICES

1 INTRODUCTION

Wetland mapping initiatives in Canada have increased in recent years leading to a plethora of scientific research and operational methodologies across a wide range of geographies, including Yukon. This is in part due to wetlands covering large portions of the landscape, their role in soil and water conservation, and susceptibility to disturbance, both anthropogenic and climatic. In addition, land use planning initiatives in Yukon in part rely on wetland maps to provide recommendations for research and management strategies for minimizing impacts to these sensitive ecosystems that will be relied on for industrial and traditional uses.

Remote sensing is the science of obtaining information about an object, area, or phenomenon by examining data acquired by a device that is not in contact with it. These devices can include, but are not limited to, satellites, aircrafts, and drones. Data is acquired by a sensor on the device that emits and/or observes how energy (i.e., electromagnetic radiation) interacts with the object, area, or phenomenon of study. Over the past 40 years, numerous satellites have been launched into orbit that provide valuable information for understanding earth processes, including wetlands. Satellites provide coarse to high spatial resolution and multispectral imagery over large areas, with minimal effort. Moreover, the availability of open-source datasets has greatly improved the efficiency and cost-effectiveness of mapping and monitoring earth systems at scale, benefitting researchers, land use planners, and policy makers. Previous wetland mapping studies completed with remote sensing technologies have established that a combination of optical, synthetic aperture radar (SAR), and topological data (e.g., Digital Elevation Models (DEM)) is the optimal technique to achieve the highest possible classification accuracy (Amani et al. 2017a, 2020; Mahdavi et al. 2018; Mahdianpari et al. 2021; Merchant et al. 2019, 2020). It has also been shown to be beneficial to derive additional features from the satellite data and include them in the classification, such as band ratios, indices, and elevation derivatives like slope, to assist in separating landcover classes. In regard to classification methodologies, it has been widely reported that an object-based classification method is superior to pixel-based techniques (Corcoran et al. 2015), especially for wetland mapping (Amani et al. 2017a, 2018b; Mahdavi et al. 2018), due to its ability to consider multiple data inputs (i.e., optical, SAR, and DEM images), capture class heterogeneity (e.g., form; graminoid, shrubby, wooded), and reduce noise (image artifacts not representing real world features), along with reported higher classification accuracies. In pixel-based classifications, each pixel is assigned a class based on that pixel's spectral properties without consideration of neighbouring pixels. However, in object-based image analysis (OBIA), pixels are grouped into objects based on spectral similarity or other external variables, such as soil or geological unit. OBIA additionally enables utilizing object spatial information and produces more proper results in terms of visual interpretations (Blaschke 2010).

Machine learning techniques have been extensively used in landcover classification where Random Forest (RF) models in particular have yielded higher accuracies compared to other commonly used machine learning algorithms, such as Support Vector Machine, Maximum Likelihood, and K-Nearest Neighbours, for wetland classification (Amani et al. 2017a; Mahdavi et al. 2018). RF is a non-parametric classifier which contains an ensemble of decision trees each of which possess several nodes dividing the input objects into mutually exclusive groups. The division continues until each node is representative of one of the final classes (Breiman 2001), and the majority result of all trees determines the class label for a particular object. RF contains several tuning parameters that are selected based on various factors, such as the number of samples, tree depth, and number of trees. A similar approach to mapping wetlands was undertaken by Ducks Unlimited Canada for the Dawson Regional

Landuse Plan. Mahdavi et al. (2018) additionally provides an extensive overview of remote sensing for wetland classification beyond what is discussed in this report.

1.1 PROJECT BACKGROUND

This report accompanies and discusses the mapping of wetland areas and adjacent non-wetland areas in the Mayo and McQuesten watersheds with particular focus on five areas of special interest: the Haggard Creek, Mayo Lake, Sprague Creek, and the Lower-South and Mid-South McQuesten sub-basins. The mapping was completed using the object-based machine learning algorithm Random Forest with multiple remote sensing datasets (i.e., Sentinel-2, Sentinel-1, ALOS PALSAR) and a DEM. The software eCognition Developer (version 10.1) was selected for use for this project as it is regarded as one of the best software for OBIA due to its ability to incorporate various types of datasets, provide a wide range of segmentation algorithms, incorporate variables such as shape, colour, texture, and contextual information in the model, and allow for the development of a knowledge base for the classification. Model training and assessment data was collected both in the field and through image interpretation. Wetland areas were classified according to the five major wetland classes of the Canadian Wetland Classification System (CWCS; National Wetlands Working Group 1997) and include shallow water (less than 2 m deep), bogs, fens, marshes, and swamps. Ecosite mapping conducted by the Government of Yukon (Environment Yukon 2019) was extensively referenced to account for wetland characteristics specific to the Yukon context. Non-wetland areas are identified as deep water (greater than 2 m deep), exposed/disturbed (e.g., rock, gravel, sand, buildings, roads, mines), forested/shrub (e.g., coniferous, broadleaf, willows, shrub birch, alder, etc.), and grassland (see ecosite BOLkp/20) (Environment Yukon 2019).

1.2 WETLAND CLASSIFICATION

Wetlands are defined by CWCS as areas that have been saturated for a prolonged period of time as to promote wetland processes as indicated by wet-adapted vegetation and hydric soils (National Wetlands Working Group 1997). The CWCS classifies wetlands into shallow water, marshes, fens, bogs, or swamps based on the characteristics of the vegetation communities and hydrology (Environment Yukon 2019; National Wetlands Working Group 1997). Shallow water systems have a water depth of less than two metres, and typically support multiple vegetation species, such as pond-lily and submerged aquatic vegetation. Marshes often form the transition between shallow water and the shoreline, and support rushes and sedges depending on water level fluctuations (Figure 1h). Swamps are periodically inundated, and the length and frequency of flooding influences the vegetation community (Figure 1i, j). Swamps can be shrub, coniferous, or broadleaf-dominated or a mixture of all three. Fens (Figure a, c, e, g) and bogs (Figure b, d, f) are peat-forming systems that support mosses, stunted vegetation, and ericaceous shrubs, and can additionally be characterized by hummocks or tussocks.

(a) Graminoid Fen

(b) Graminoid Bog

(c) Shrubby Fen

(d) Shrubby Bog

(e) Wooded, coniferous Fen

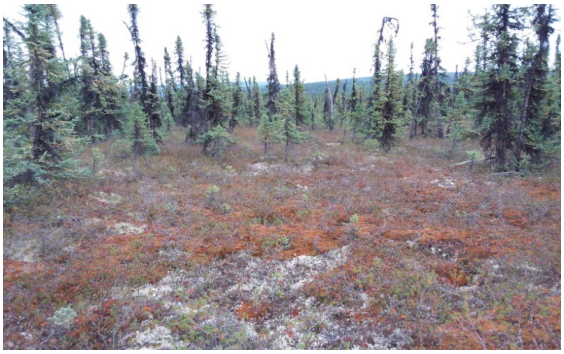

(f) Wooded, coniferous Bog

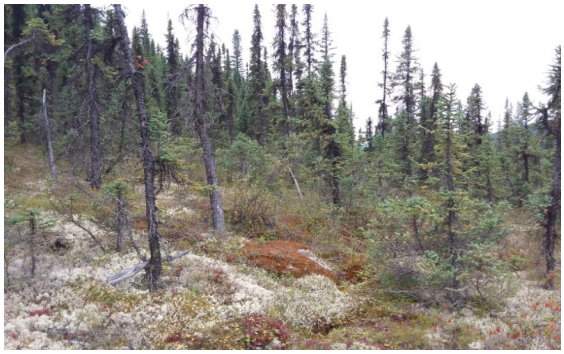

(g) Wooded, coniferous Fen

(h) Graminoid Marsh

(i) Shrubby Swamp

(j) Wooded, coniferous Swamp

Figure 1: Photos of field sites, collected by WSP during the August 2021 field survey, representing some of the wetland forms found within the Mayo and McQuesten watersheds

While large wetland complexes are most commonly found on level terrain, due to the permafrost conditions wetlands in Yukon can also occur on northern aspects and riparian drainages of various elevation and slope (Figure 1g). This is the result of frozen ground conditions impeding near-surface soil drainage, promoting the establishment of the wet-adapted vegetation and altered soils which characterize wetlands (National Wetlands Working Group 1997). Thermokarst wetlands, formed from a degradation in the underlying permafrost, are also present (Figure 1b). Additionally, in Yukon, peat deposits with a depth greater than 30 cm are considered peatlands if other indicators are present (CryoGeographic Consulting 2018; Environment Yukon 2019) as opposed to the greater than 40 cm depth cut-off described in the CWCS (National Wetlands Working Group 1997).

1.3 STUDY AREA

The Mayo and McQuesten watersheds (7,508 km^2) and the five areas of special interest (2,495 km^2) are located in central Yukon territory and situated within the McQuesten Highlands and Yukon Plateau North ecoregions of the Boreal Cordillera ecozone (Figure 2). Mean annual temperature is approximately -5°C and varies by elevation, which ranges from 320 to 2,160 m above sea level. Precipitation is moderate with annual amounts of 300 mm to 600 mm (Yukon Ecoregions Working Group 2004, p. 197-206).

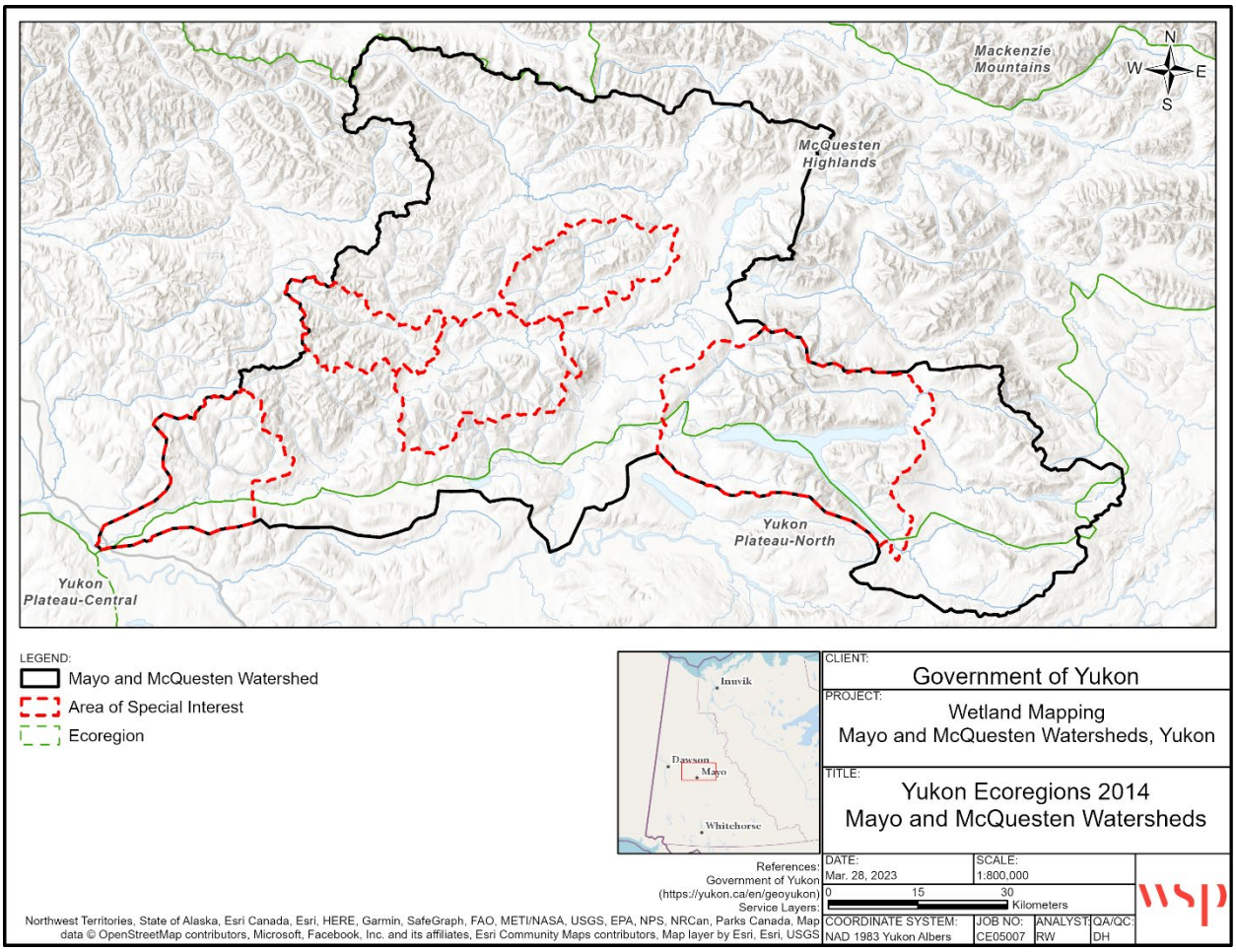

Figure 2: Ecoregions found within the Mayo and McQuesten watersheds

Permafrost is common throughout the study area where valley floors host discontinuous permafrost in silty sediments overlain by organic deposits. Near surface ground temperatures in permafrost soils have been reported between -1.3°C and -1.8°C near Mayo. Valley soils are often a mixture of glacial parent materials and include coarse-textured well-drained Eutric Brunisols and imperfectly drained Turbic Cryosols. Black and white spruce forests dominate at mid to low elevations which transition to willows and ericaceous shrubs in the subalpine (Environment Yukon 2019). Mixed canopy forests are frequent in areas following forest fires. Sage grasslands and aspen stands occur on steep, south-facing slopes. Shrublands can occur extensively at mid elevations and valley bottoms due to cold air drainage. Wetlands are primarily found in the lower portions of larger river valleys (e.g., McQuesten River), but are also found on northern aspects and drainages at higher elevations or steeply sloping terrain. Wetlands are generally characterized by willows, sedges, stunted black spruce, and sphagnum and/or brown moss.

2 DATASETS

2.1 FIELD SURVEY AND INTERPRETED DATA

Field data was collected by Government of Yukon ELC staff from 07 to 11 July and 30 July to 09 August 2021 and by WSP between 17 to 21 August 2021 throughout the Mayo and McQuesten watersheds in 20 m diameter plots (Figure 3). Survey data collected included GPS location, descriptions of site dominant vegetation, soils, landscape position, depth to permafrost, pH (using a Hanna Instrument pH/conductivity/TDS tester model HI98129 where applicable), photos, and preliminary ecosite association, and included both wetlands and non-wetlands. In some cases, sites with less than 30 cm of peat were considered peatlands if seasonal frost was located at or immediately adjacent to the peat-mineral interface when supported by vegetation indicators. This was because functionally the water column was within peat even though the peat was only 30 cm deep. Field forms were reviewed for accuracy by professionals experienced in wetland and vegetation classification and were subsequently entered into the Yukon Biophysical Information System (YBIS). In total, 56 and 34 sites were completed by Government of Yukon and WSP, respectively, and wetland classes from both sets of data were compared and reviewed by a WSP vegetation and wetland specialist. WSP captured eight additional sites where an ecosite was visually determined without the completion of a survey. This was done to note characteristic sites during the course of fieldwork where a survey was not needed due to the obvious class, proximity to a site where a survey was completed, or to ensure more important locations were visited. As a survey was not conducted, these sites were not inputted into YBIS. A summary of the collected field data used in the classification is displayed in Table 1. A total overall number of field sites collected by Government of Yukon and WSP was 99.

Table 1: Summary of the Collected Field Data by Government of Yukon and WSP, and Sites Interpreted from Satellite Imagery. Half (50%) of the Total Samples per Class were Randomly Selected as Training Data and the Remaining Half (50 %) used for Accuracy Assessment

LANDCOVER	NO. FIELD SITES[1]	NO. INTERPRETED SITES[2]	TOTAL NUMBER OF SAMPLES[3]	TOTAL SAMPLE AREA (km²)
Shallow water	–	11	11	0.38
Marsh	7	24	31	0.54
Swamp	16	41	57	0.28
Fen	24	92	116	2.14
Bog	11	29	40	0.60
Deep water	–	17	17	21.75
Exposed/disturbed	–	33	33	2.08
Forested/shrub	40	135	175	10.90
Grassland	1	2	3	0.05
Total	**99**	**384**	**483**	**38.72**

Notes:

[1] Field Sites collected by Government of Yukon and WSP.

[2] Interpreted from satellite imagery.

[3] Samples split for training data and classification accuracy assessment.

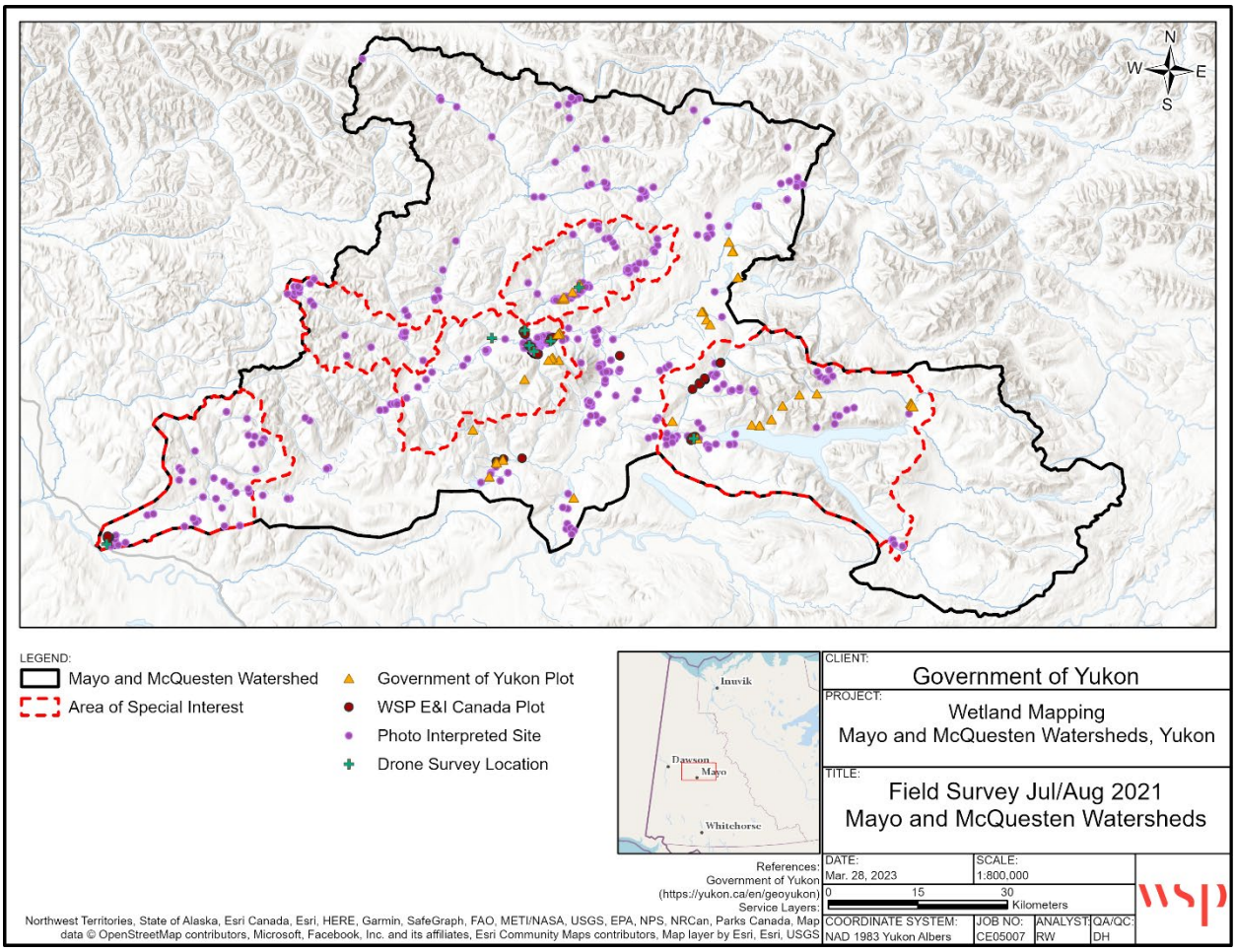

Figure 3: The project area and the distribution of field data, which were collected by Government of Yukon and WSP during July and August 2021, as well as the location where drone imagery was acquired and interpreted sites

The GPS locations for the in-situ field data were then used to manually delineate polygons representative of the assigned class at a scale of 1:10,000 for use in the OBIA. This scale was chosen based on mapping scale recommendations in Environment Yukon (2016, p. 21) for local ecosystem mapping. Field data was collected in 20 m diameter plots, and as such in cases where the ecosite boundaries were not obvious in the satellite imagery the delineated polygons were purposefully kept smaller to ensure they represented the surveyed ecosite.

Additional polygons were manually delineated and interpreted from high-resolution satellite imagery available through Government of Yukon (SPOT 6/7), Esri (World Imagery Basemap), and drone imagery by an experienced remote sensing analyst. Interpreted sites were assigned a landcover class (i.e., classes listed in Table 1) based on spectral signature, general vegetation, and landscape position. For example, in high resolution imagery bogs typically appear as sparse treed forests with a mix of white (lichen) and orange (Sphagnum) coloured ground covers. In a Sentinel-2 imagery false colour composite, where the Red channel represents the NIR band, Green represents the SWIR1, and Blue represents the Red band, bogs typically appear bright pink (high Sphagnum coverage) to violet-brown (lichen and spruce). Care was taken to only select interpreted sites where the analyst had high confidence in the call based on a variety of the aforementioned characteristics and avoided fuzzy wetland boundaries to promote spectral purity in the training and

assessment data. However, swamps and shallow water can be difficult to interpret from satellite imagery with certainty due to at times being unable to see the key indicators of these classes (e.g., water depth, hummocky landform, hydric soils).

During the segmentation processes, discussed later in this report (see section 3.1), the segmentation algorithm was parameterized to create segments that perfectly aligned with the delineated polygons to ensure no segments were used to train the model that were not within the manually delineated boundaries and to avoid boundary misalignment due solely to the difference in spatial resolution (i.e., boundaries visible in 1.5 m SPOT imagery versus 10 m Sentinel-2 imagery). However, the segmentation algorithm was not prevented from subdividing the input polygons into smaller segments, thus a delineated polygon could contain multiple segments. This allowed the segmentation process to identify site heterogeneity (e.g., separate inundated versus vegetated portions of a patterned fen), and provided a range of class spectral variance for the model to be trained on. The finer segmentation scale additionally increased the number of training polygons used in model training and addressed the variance in the size of the delineated site polygons (i.e., by subdividing into smaller segments based on a scale parameter). Field and interpreted polygons were combined and randomly split approximately 50/50 per class into model training and assessment datasets.

2.2 SATELLITE DATA

It is well accepted that the fusion of optical, SAR, and DEM data is the optimal combination for wetland mapping with the highest possible classification accuracy (Mahdavi et al. 2018). In this project, Sentinel-2, Sentinel-1, ALOS PALSAR, and DEM data (Figure 4) were the primary inputs applied to classify wetlands in the Mayo and McQuesten watersheds. A brief description of each dataset and the related processing is provided in the following subsections. A full list of imagery used is presented in Appendix A.

2.2.1 SENTINEL-2

Sentinel-2 is an optical (multispectral) satellite operated by the European Space Agency. It has been operating since 2015 with a spatial resolution of 10 to 20 m for the optical spectral bands and a revisit time of five days (Table 2). Due to Sentinel-2's higher spatial (i.e., size of a pixel), temporal (i.e., the time it takes for the satellite to pass over the same location), and spectral (i.e., number of bands the sensor measures) resolutions compared to other open-access satellite data (e.g., Landsat imagery), it is frequently used for landcover classification. The greater spatial and spectral resolutions allow for better discrimination between landcover classes, and the greater temporal resolution increases the chances of capturing cloud-free scenes, facilitating wetland monitoring. In addition, unlike other similar space-based optical sensors, Sentinel-2 includes three red edge bands, which have been shown to have a high potential for wetland discrimination (Ozesmi and Bauer 2002; Adam et al. 2010; Mahdavi et al. 2018; Amani et al. 2018a). Sentinel-2 imagery has previously been used to map wetlands in Yukon (Merchant et al. 2019) and across Canada (Mahdianpari et al. 2021).

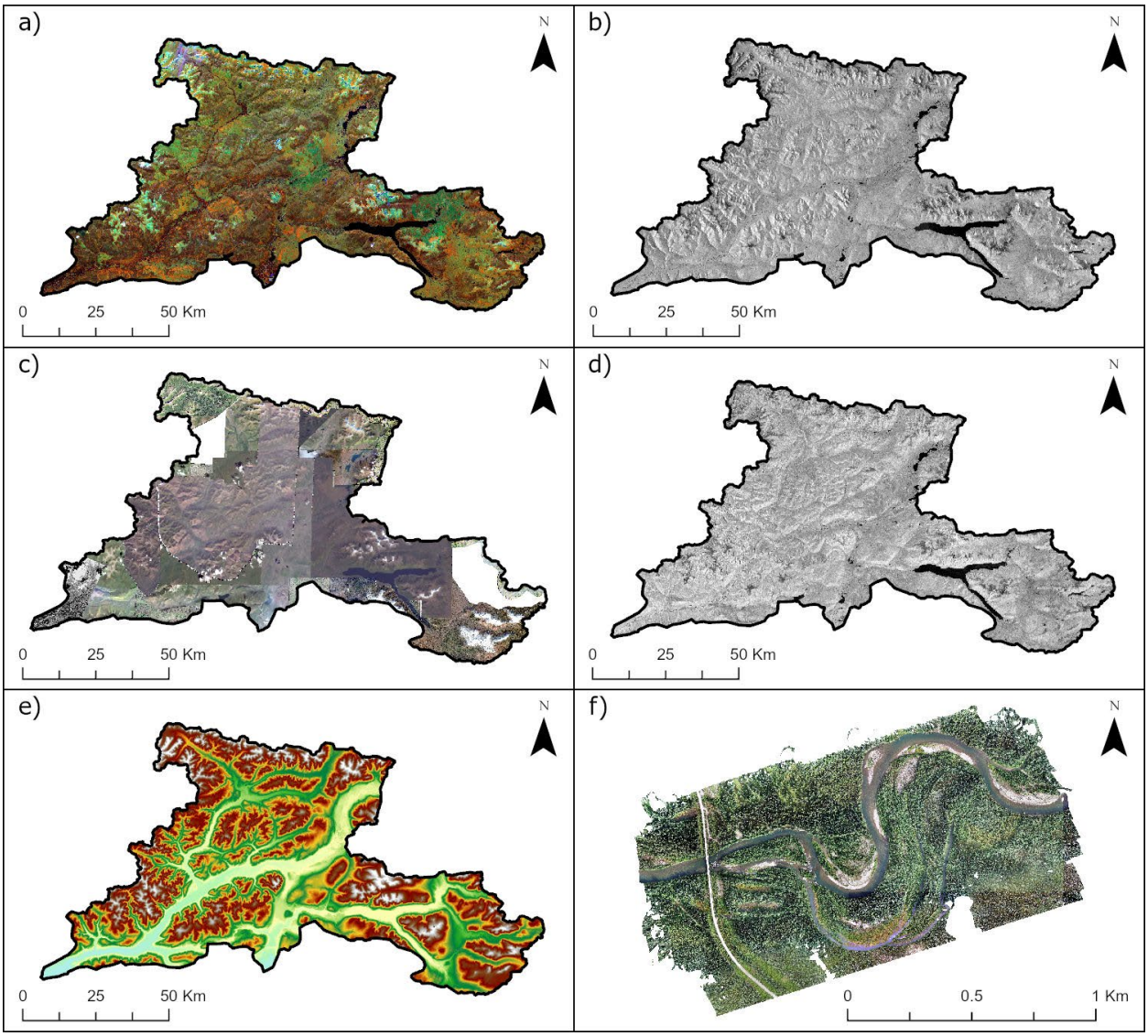

Figure 4: **Satellite imagery used in the wetland classification of the project area: a) Sentinel-2 (Red: NIR, Green: SWIR1, Blue: Red), b) Sentinel-1 (VH polarization), c) SPOT 6/7 (8 bit), (d) ALOS PALSAR (HV polarization), e) merged CDEM and ArcticDEM, and f) a drone orthomosaic for one of the flight locations (McQuesten River (Hwy 2) site)**

Table 2: Sentinel-2 Bands used for Classifying Wetlands in the Project Area and their Central Wavelengths and Resolutions

BAND NAME	CENTRAL WAVELENGTH (µm)	SPATIAL RESOLUTION (m)
Blue	0.490	10
Green	0.560	10
Red	0.665	10
Red Edge 1 (RE1)	0.705	20
Red Edge 2 (RE2)	0.740	20
Red Edge 3 (RE3)	0.783	20
Near Infrared (NIR)	0.842	10
Narrow Near Infrared (NNIR)	0.865	20
Shortwave Infrared 1 (SWIR1)	1.610	20
Shortwave Infrared 2 (SWIR2)	2.190	20

Atmospherically corrected surface reflectance images (i.e., images that have been adjusted for weather and other atmospheric effects; for details see https://sentinel.esa.int/documents/247904/685211/Sentinel-2_User_Handbook) from Sentinel-2 (Level-2A; ee.ImageCollection ("COPERNICUS/S2_SR")) were acquired from Google Earth Engine (GEE). Images with less than 5% cloud cover in July and August between 2018 and 2021 (18 images total, see Appendix A) were selected and a median reducer function (ee.Reducer) was applied to the image stack. This approach was used to create a single composite image containing the median of the pixel values, within the given timeframe, with no/least possible cloud and snow covers. This approach also removed very dark (i.e., shadow) and very bright (e.g., haze, cloud, snow) pixels. Cloud and snow masking is an important pre-processing step in areas such as Yukon due to the predominantly unfavorable weather conditions, particularly in the mountainous regions where cloud and snow cover are frequent. Cloud and snow effectively mask the spectral signatures of the underlying landcover making it challenging or impossible to map correctly. While studies have shown that multi-season optical image is beneficial for landcover mapping due to the ability to discriminate between broadleaf and coniferous species, visual observation of Sentinel-2 images outside July and August revealed the mountainous areas to be impacted by snow cover. As such, multi-temporal images were not utilised in this project. All Sentinel-2 spectral bands in the final mosaic were resampled to 2 m resolution to match the DEM and projected to WGS 84 UTM Zone 8N.

2.2.2 SENTINEL-1 AND ALOS PALSAR

The inclusion of SAR imagery has been shown in numerous studies to improve wetland classification (Amani et al. 2017a; Amani et al. 2018b; Amani et al. 2019; Merchant et al. 2019; Adeli et al. 2020; Merchant et al. 2020). SAR sensors measure the backscatter of emitted microwave energy in different polarizations of a single band which influences the ability of the radar signal to penetrate a medium and how it interacts with the surface. For example, C-band has low to moderate penetration and is typically used for landcover mapping and ice and shoreline detection. L-band radar uses a longer wavelength compared to a C-band SAR systems, and thus can increase the ability to penetrate forest cover compared to C-band. As such, L-band sensors are often used for biomass and vegetation mapping. SAR sensors also emit and receive energy in horizontal (denoted by a 'H') or vertical (denoted by a 'V') polarizations. Each polarization carries information about the imaged surface. For example, rough surfaces

such as bare soil or water are most sensitive to VV polarization, forest canopies are sensitive to VH and HV, and inundated vegetation is sensitive to HH. Additionally, SAR sensors can capture images through clouds. For this project, imagery from Sentinel-1 (C-band; VV and VH polarizations) and ALOS PALSAR (L-band; HH and HV polarizations) were utilized to combine the benefits of C- and L-band, and multiple polarizations (Table 3).

Table 3: Band, Polarization, and Resolution of Sentinel-1 and ALOS PALSAR Imagery used for Classifying Wetlands in the Project Area

PLATFORM/SENSOR	CENTRAL WAVELENGTH (µm)	POLARIZATION	SPATIAL RESOLUTION (m)
Sentinel-1	5.405 GHz (C-band)	VV, VH	10
ALOS PALSAR	1.270 GHz (L-band)	HH, HV	20

In this project, pre-processed Sentinel-1 imagery (C-band, 5.405 GHz) in VV and VH polarizations were acquired from GEE (ee.ImageCollection ("COPERNICUS/S1_GRD")) from July to August 2020 (11 images total, see Appendix A) in an ascending satellite orbit as Ground Range Detected (GRD) scenes (for pre-processing steps see https://developers.google.com/earth-engine/guides/sentinel1). The pre-processed imagery was mosaicked, and a mean filter (30 m radius) applied to minimize additional remaining noise and the inherent salt and pepper texturing in the data. The Sentinel-1 mosaic, for both VV and VH polarizations, was resampled to 2 m resolution to match the DEM and projected to WGS 84 UTM Zone 8N.

Pre-processed ALOS PALSAR scenes (L-band, 1.27 GHz) were acquired from the Alaska Satellite Facility (ASF) from July and August 2008 to 2010 (9 images total, see Appendix A) in an ascending satellite orbit in Fine Beam Dual (FBD) polarization mode at HH and HV polarizations (for pre-processing steps see https://asf.alaska.edu/data-sets/sar-data-sets/alos-palsar). The pre-processed imagery was mosaicked, and a 3x3 boxcar filter applied filter to minimize noise and the inherent salt and pepper texturing in the data. Values were converted to decibels to match the Sentinel-1 imagery. The imagery was mosaicked in ArcGIS and resampled to 2 m spatial resolution to match the DEM and projected to WGS 84 UTM Zone 8N for both the HH and HV polarizations.

ALOS PALSAR imagery was used over the available PALSAR-2 yearly mosaic as the yearly mosaic is compiled using scenes preferentially selected based on their minimal response to soil moisture which makes the imagery less ideal for wetland mapping. The yearly mosaic may also include scenes from the winter months with frozen and/or snow-covered vegetation. It should be noted that the ALOS satellite was decommission in early 2011 thus summer imagery after the 2010 season cannot be obtained, and individual scenes, which could be selected for optimal timing, from its successor mission ALOS PALSAR-2 were not available to WSP at the time of this project.

2.2.3 SPOT 6/7

SPOT6/7 satellites are commercial high-resolution satellites (1.5 m spatial resolution) that provide detailed imagery in the red, green, blue, and NIR bands. Near full-coverage of SPOT6/7 imagery was provided for the Mayo and McQuesten watersheds as 8-bit RGB, RGB-NIR, or panchromatic scenes. While Amani et al. (2020) found that the inclusion of high-resolution imagery improved the delineation of small landscape features, upon review of the SPOT 6/7 imagery it was determined that some of the images were too cloudy and would decrease classification accuracy. As well, the variability in available bands, lower bit- depths (8 bit vs 16 bit), and incomplete coverage of the study area contributed to the decision to omit the SPOT imagery from segmentation and classification. Instead, the SPOT imagery, in combination with high-resolution Esri World Imagery Basemap available through ArcGIS, was used to supplement the YBIS plot data through visual interpretation by WSP vegetation and wetland specialists.

2.3 TOPOGRAPHIC DATA

Topographical products provide valuable information on elevation, landscape features, and vegetation structure and height, and have been used successfully for wetland mapping (Amani et al. 2020; Millard and Richardson 2013; O'Neil et al. 2018). This is largely because most wetlands form on level to gently sloping terrain, within topographical depressions, or where other conditions allow the water table to reside near the surface (National Wetlands Working Group 1997). However, elevation data on its own does not necessarily assist in separating wetland classes. For example, swamps can occur in both low and high elevation drainages. Elevation derivatives have been shown to capture the spatial patterns that characterize saturated areas, such as the propensity of a site to be wet (O'Neil et al. 2018). Table 4 describes the elevation derivatives used in this study and the rational for their inclusion.

Table 4: Topographical Derivatives used for Classifying Wetlands in the Project Area Derived from the Merged CDEM and ArcticDEM Datasets

DERIVATIVE	RATIONAL
Height Above Nearest Drainage	Related to local draining potential and water table depth which are relevant factors in wetland formation (Nobre et al. 2011)
Aspect	Certain aspects (e.g., steep north vs. south slopes) in the study area have differing vegetation communities (e.g., coniferous vs. sage grassland) (Environment Yukon 2019)
Slope	Wetlands generally occur on level to gently sloping terrain (Environment Yukon 2019; National Wetlands Working Group 1997)
Profile Curvature	Curvature of a slope effects erosional and depositional processes (Moore et al. 1991), and may relate to soil formation and hydrological processes
Plan Curvature	Curvature of a slope effects flow divergence and convergence (Moore et al. 1991), and may relate to water accumulation

In this project, a combination of the Canadian Digital Elevation Model (CDEM) and ArcticDEM topographic data were used. CDEM for Yukon is available from the GeoYukon portal at a 30 m spatial resolution. The CDEM is derived from existing Canadian Digital Elevation Data which were extracted from the hypsographic and hydrographic elements of the National Topographic Data Base at the scale of 1:50 000, the Geospatial Database, various scaled positional data acquired by the provinces and territories, or remotely sensed imagery (Natural Resources Canada 2013). The CDEM dataset was resampled and merged with the ArcticDEM (2 m spatial resolution) which is derived from high resolution optical stereo imagery (Porter et al. 2018). The ArcticDEM covered approximately 98% of the study area and the CDEM was used to fill data gaps (2% of the total merged DEM area). The resultant dataset is a surface model reflecting both bare earth and terrain features at 2 m spatial resolution and projected to WGS 84 UTM Zone 8N. The optical and SAR imagery were resampled to 2 m to match the DEM resolution to try and capture small topographical features (e.g., drainages, changes in slope or curvature) where wetlands may occur in the Mayo and McQuesten watersheds. Elevation derivatives, including the aspect, slope, height above nearest drainage (based on the 50k watercourse and waterbody Canvec datasets), as well as profile and plan curvature topographic products were generated in ArcGIS Pro (version 2.9) from the merged DEM for use in the classification.

2.4 DRONE IMAGERY

Drone imagery was acquired with a Phantom 4 Pro drone over five locations (Figure 3) coincident with field plot data collection by WSP between 17 to 21 August 2021. Flight locations were selected based on accessibly, availability of legal flying conditions (e.g., clear line of sight), control points, wetland abundance, and proximity to surveyed field sites. Where possible, multiple field sites were sampled within the same area that was being surveyed by the drone. Collected imagery was subsequently processed and mosaicked. DEMs were additionally produced for each site based on image overlap. A detailed report on processing parameters, registration, and calibration are included with the imagery files. Table 5 summarizes the five flights and produced imagery.

Table 5: Summary of the Drone Flights and the Captured Orthomosaicked RGB Imagery

SITE	APPROX. LOCATION	NUMBER OF IMAGES	FLYING ALTITUDE	GROUND RESOLUTION	COVERAGE AREA	NO. CONTROL POINTS
Mayo River	-135.45 °W, 63.77 °N	761	129 m	3.21 cm/px	1.29 km^2	7
Victoria Mine Rd (km 21.5)	-136.00 °W, 63.88 °N	1,158	136 m	3.37 cm/px	1.62 km^2	4
Victoria Mine Rd (km 25.8)	-136.04 °W, 63.92 °N	1,094	141 m	3.52 cm/px	1.3 km^2	3
Victoria Mine Rd (km 18.5)	-135.95 °W, 63.90 °N	1,633	143 m	3.48 cm/px	1.9 km^2	7
Victoria Mine Rd (km 23)	-136.03 °W, 63.89 °N	1,623	135 m	3.27 cm/px	1.74 km^2	7
McQuesten River (Hwy 2)	-137.41 °W, 63.55 °N	1,469	130 m	3.14 cm/px	1.45 km^2	5

Due to the minimal coverage of drone imagery across the entire Mayo and McQuesten watersheds, the imagery was not included in the segmentation or classification. Instead, the images were used to interpret additional training and assessment data. The high spatial resolution (approximately 3.5 cm) allowed the interpreter to visually confirm species presence and ground conditions (e.g., hummocks, tussocks, inundation, etc.) and assign a class with increased confidence than with SPOT6/7 imagery alone. As such, a greater number of interpreted sites were concentrated in these areas.

3 METHODOLOGY

3.1 SEGMENTATION

The multi-resolution segmentation algorithm (Baatz 2000), available in the eCognition software, was used to segment the imagery into meaningful objects. This algorithm is a bottom-up region merging technique that groups neighboring pixels based on the homogeneity criteria. Segmentation was performed using the Sentinel-2 red, green, blue, NIR, and SWIR bands to take advantage of the native 10 m spatial resolution bands (i.e., red, green, blue) for discerning greater detail, and the sensitivity of NIR and SWIR to vegetation and water Segment size is controlled by the scale parameter, where higher values result in the algorithm producing larger objects. After assessing two different levels, a final scale value of 200 was used to produce then initial classification, and a value of 50 used for finishing refinements. The large-scale segmentation was used to develop the initial wetland versus non-wetland classification, and the smaller scale segmentation used to produce the map of the five wetland and four non-wetland classes. The shape (deviation from a compact or smooth shape) and compactness (border length divided by area) parameters were given values of 0.1 and 0.9, respectively, based on trial and error until satisfactory results were achieved. As mentioned in section 2.1, the segmentation was constrained by the training polygons, such that created segments that overlapped the delineated training polygons had the same bounding geometry though could contain several smaller segments.

3.2 SEGMENT STATISTICS

In OBIA, the classification model is trained and applied based on a series of statistics describing each segment (e.g., mean and standard deviation pixel value per segment per spectral band). A common approach to improve model accuracy is by extracting and including additional features, such as band ratios and indices for optical imagery (Amani et al. 2019) and co- (i.e., same sent and received; VV or HH) and cross- (i.e., different sent versus received; VH or HV) polarizations for SAR imagery (Mahdavi et al. 2018). Based on previous studies (Amani et al. 2017a; Amani et al. 2018a,b; Mahdavi et al. 2017; Mahdavi et al. 2018), the features and indices listed in Table 6 were used in the classification as they had the highest potential to discriminate various wetland classes.

Table 6: Bands, Indices, Ratios, and Other Features used Included in the Object-Based Random Forest Model

PLATFORM	MODEL INPUT	EQUATION/DESCRIPTION
Sentinel-2	Blue	Segment mean
	Green	Segment mean
	Red	Segment mean
	Red Edge-1	Segment mean
	Red Edge-2	Segment mean
	Red Edge-3	Segment mean
	NIR	Segment mean
	Narrow NIR	Segment mean
	SWIR-1	Segment mean

PLATFORM	MODEL INPUT	EQUATION/DESCRIPTION
	SWIR-2	Segment mean
Sentinel-1	VV	Segment mean
	VH	Segment mean
ALOS PALSAR	HH	Segment mean
	HV	Segment mean
DEM	Elevation	Segment mean
	Height Above Nearest Drainage (HAND)	Segment mean
	Aspect	Segment mean
	Slope	Segment mean
	Profile Curvature	Segment mean
	Plan Curvature	Segment mean
Index	Normalized Differential Vegetation Index (NDVI)	(NIR-Red)/(NIR+Red)
	Normalized Differential Water Index (NDWI)	(Green-NIR)/(Green+NIR)
Ratio	Sentinel-1 Ratio	VH/VV
	ALOS PALSR Ratio	HV/HH
	Textural features	band standard deviation
	Geometry features	object compactness

3.3 OBJECT-BASED RANDOM FOREST CLASSIFICATION

Thresholding techniques were used to mask area that were likely non-wetlands, such as mountain crests and human development (e.g., roads, buildings), as previous mapping experience showed that the RF algorithm sometimes confused sparse alpine vegetation with the fen and marsh wetland classes. The thresholding was done by assessing the natural breaks in the height above nearest drainage derivative to determine the vertical distance above the nearest mapped drainage in which wetlands were likely not to form based on visual inspection. Anthropogenic disturbances, such as mines, roads, and buildings were masked using the Brightness statistic in eCognition (the sum of all input layers divided by the number of input layers) and manual methods. Following masking, the RF algorithm was trained using a random selection of 50% of the field and interpreted polygons (i.e., training samples) while the remaining 50% were used for the accuracy assessment (i.e., test samples). Objects were assigned a class based on the majority result of all the decision trees created as part of the RF model for that object.

The final map was then converted from raster to vector format and reviewed at a scale of 1:10,000 for further refinement. As the segmentation was performed on medium-resolution imagery the resultant objects did not always perfectly align with actual landcover boundaries, especially if the objects represented small landscape features or transitional classes. The polygon refinement process allowed for the modification of wetland polygons to better capture feature boundaries and correct any additional errors. The refined map was used as the basis of a second segmentation at the finer 50 scale (i.e., was used to constrain the segmentation) where non-wetland areas were classified and additional refinements to wetlands areas were completed. The final classification was produced in raster format at 10 m spatial resolution and the WGS 84 UTM Zone 8N projection.

3.4 ACCURACY ASSESSMENT

Accuracy assessments compare the classification with field data to provide information on the overall accuracy and reliability of the map, as well as to understand classification errors (Gopal and Woodcock 1992). Two types of accuracy assessments were conducted for the produced Mayo and McQuesten wetland classification: visual and statistical accuracy assessments.

A simple, but effective type of accuracy assessment is visual inspection. For a visual accuracy assessment, the classification is analysed and interpreted visually using high spatial resolution images (e.g., Esri World Imagery Basemap available in ArcGIS) to see if the mapped classes visually correspond to real features on-the-ground.

Classification accuracy is also statistically assessed through an error matrix using the test samples (see Table 7 as an example). An error matrix is an array with columns representing the assessment data (i.e., samples) and the rows representing the classification data (i.e., mapped class). The numbers within the matrix represent the number of sites assigned to a certain class, where numbers along the main centre diagonal (highlighted cells in Table 7) indicate correctly classified polygons. Numbers in the off-diagonal cells (non-highlighted cells) indicate incorrectly classified polygons and, therefore, potential errors in the map. Overall accuracy (OA) is calculated as the sum of the correctly classified polygons divided by the total number of assessment polygons. Producer's accuracy (PA) is calculated by dividing the total number of polygons correctly classified for a particular class by the total number of assessment polygons for that class and represents polygons that are not classified as the same class as the assessment polygon. User's accuracy (UA) is calculated by dividing the total number of polygons correctly classified for a particular class by the total number of sites classified as that class. This represents polygons that have been assigned a class they do not belong to. It is also important to consider that a polygon may been assigned to the correct class purely by chance. To accommodate for this degree of chance, Cohen's Kappa coefficient is also calculated from the error matrix (Cohen 1960). The Kappa coefficient is a statistic that indicates if the error matrix is significantly different from a random classified result, where values close to 1 indicate a strong agreement between the classified output and the assessment data, and values close to 0 indicate poor agreement.

Table 7: Example Confusion Matrix

MAPPED CLASS	SAMPLES					
		CLASS A	**CLASS B**	**CLASS C**	**ROW TOTAL**	**UA**
	Class A	20	1	-	21	20 ÷ 21 = 95%
	Class B	2	10	1	13	10 ÷ 13 = 77%
	Class C	-	1	15	16	15 ÷ 16 = 94%
	Column Total	22	12	16	50	
	PA	20 ÷ 2 = 91%	10 ÷ 12 = 83%	15 ÷ 16 = 94%		OA = 90%

4 RESULTS

4.1 MAYO AND MCQUESTEN WATERSHEDS CLASSIFICATION

The produced map (Figure 5) identified overall wetland extent across the Mayo and McQuesten watersheds, and subsequently mapped five wetland classes of shallow water, marsh, swamp, fen, and bog. The non-wetland areas were broadly classified as either uplands (i.e., exposed/disturbed, forested/shrub, grassland) or deep water. Figure 6 highlights two areas in greater detail. The produced map showed that wetlands cover approximately 540 km^2 (7%) of the study area of which fen is the most common wetland class, constituting 364 km^2 (5%). Shallow water covered the least amount of the study area with approximately 14 km^2 (<1%) mapped in the produced classification. Marsh and bog coverages were similarly low with approximately 16 km^2 (<1%) and 23 km^2 (<1%), respectively. Table 8 reports the coverage of all wetland and non-wetland classes within the Mayo and McQuesten watersheds. Of the wetland classes, fens constituted approximately 67%, followed by swamps (23%), bogs (4%), and marsh and shallow water (approximately 3% each).

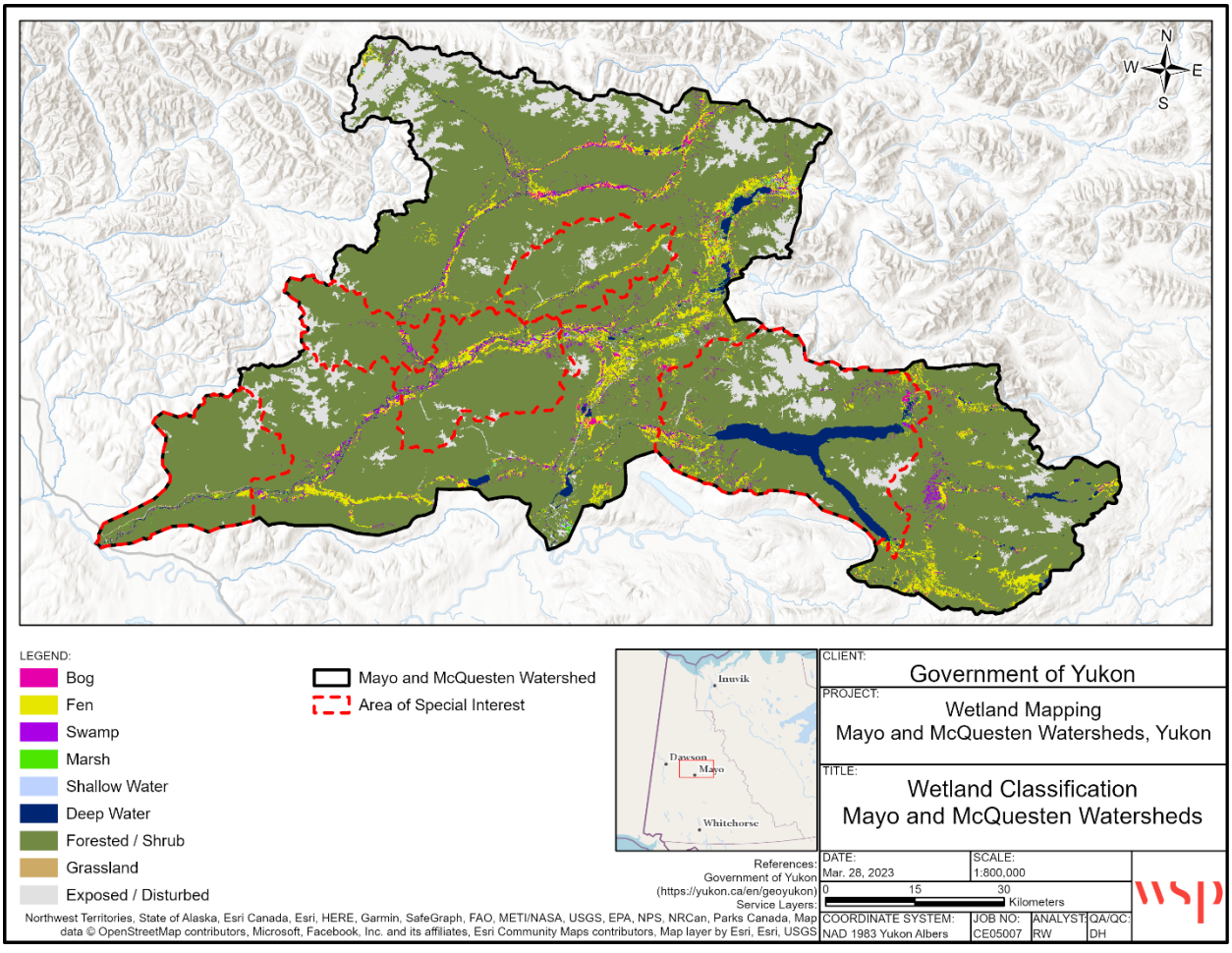

Figure 5: **Overview of the produced classification depicting wetland and non-wetland areas within the Mayo and McQuesten Watersheds**

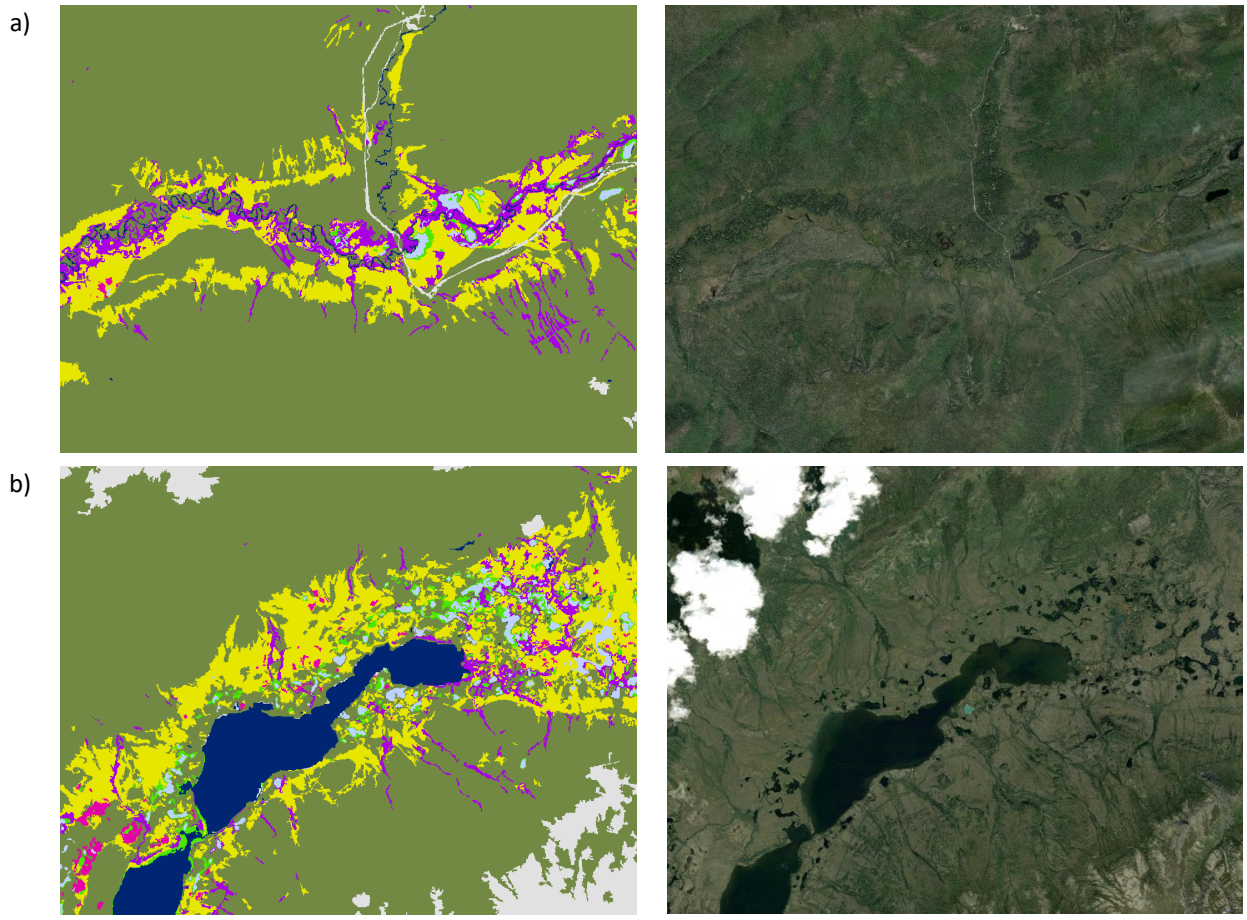

Figure 6: **Classification examples at a 1:50,000 scale (left) compared to the satellite imagery (right). Example a) is the McQuesten River along Victoria Mine Road, and b) is in the northeast portion of the project area near the Beaver River Planning Area.**

Table 8: **Area and Percent of the Mayo and McQuesten Watersheds Occupied by Different Wetland and Non-wetland Classes**

CLASS	AREA (km²)	% OF STUDY AREA
Wetland		
Shallow water	13.68	0.18
Marsh	16.00	0.21
Fen	364.28	4.85
Bog	23.32	0.31
Swamp	123.61	1.65
Total (Wetland)	*540.88*	*7.20*
Non-wetland		
Deep water	158.14	2.11
Exposed/disturbed	730.34	9.73
Forested/shrub	6,077.07	80.93
Grassland	1.91	0.02

Total (Non-wetland)	*6,967.46*	*92.80*
Grand Total	**7,350.2**	**100.0**

The majority of the wetlands were mapped along major rivers and notable valleys, such as along the McQuesten and Mayo Rivers. Fens and bogs were most commonly found on gently sloping to level terrain in the valley bottoms, while swamps often occupied lower toe-slopes, mid-slope drainages, and shorelines. Marshes and shallow waters (<2 m) were similarly associated with valley bottoms and within peatland complexes. Non-wetland areas were primarily composed of a variety of upland ecosites. Deep water, which consisted of deep (>2 m water depth) ponds and lakes as well as flowing water, composed approximately 2% of the study area and occurred in valley bottoms along with wetlands.

4.2 CLASSIFICATION WITHIN THE AREAS OF SPECIAL INTEREST

Within the five areas of special interest (Figure 7), wetlands cover approximately 115 km^2 (5%) of the areas of special interest of which fen is similarly the most common wetland class, constituting 70 km^2 (3%). Shallow water covered the least amount of area within the sub-basins with approximately 2 km^2 (<1%) mapped in the produced classification. Marshes covered approximately 4 km^2 (<1%), bogs covered 3 km^2 (<1%), and swamps covered 36 km^2 (1%). Table 9 reports the coverage of all wetland and non-wetland classes within the Mayo and McQuesten areas of special interest as a whole. Of the wetland classes, fens constituted 61%, followed by swamps (31%), marsh (3%), bog (2%) and shallow water (approximately 1%). Table 10 reports the coverage of all wetland and non-wetland classes for each of the individual areas of special interest.

Table 9: Area and Percent of the Mayo and McQuesten Areas of Special Interest Occupied by Different Wetland and Non-wetland Classes

CLASS	AREA (km^2)	% OF STUDY AREA
Wetland		
Shallow water	1.65	0.07
Marsh	3.92	0.16
Fen	70.30	2.83
Bog	3.17	0.13
Swamp	35.63	1.43
Total (Wetland)	*114.68*	*4.60*
Non-wetland		
Deep water	108.35	4.34
Exposed/disturbed	208.91	8.38
Forested/shrub	2,059.33	82.60
Grassland	1.91	0.08
Total (Non-wetland)	*2,378.5*	*95.40*
Grand Total	**2,493.18**	**100.0**

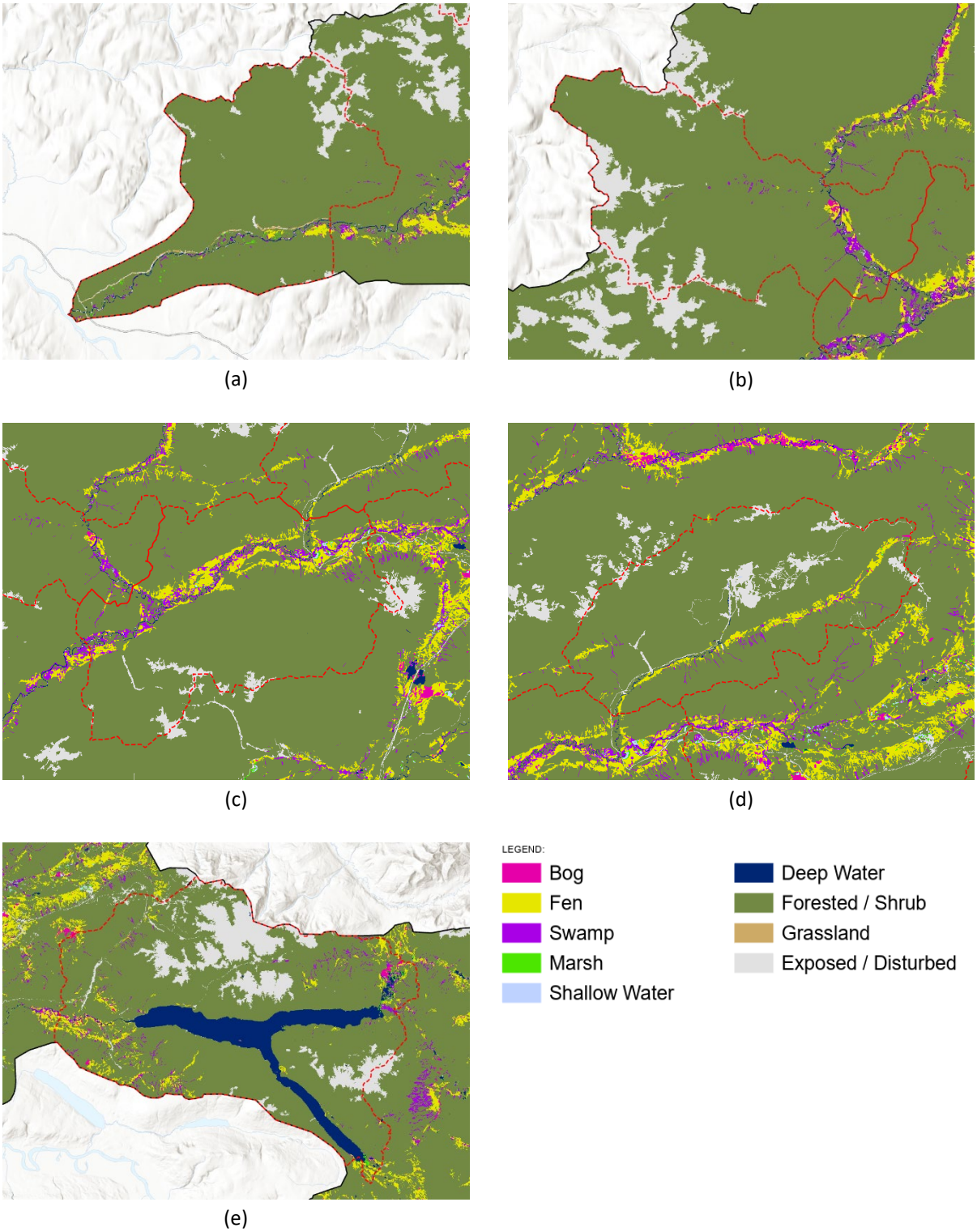

Figure 7: **Overview of the produced classification depicting wetland and non-wetland areas within the areas of special interest: a) Lower South McQuesten, b) Sprague Creek, c) Mid South McQuesten, d) Haggard Creek, and e) Mayo Lake**

Table 10: Area and Percent of Each of the Five Areas of Special Interest Occupied by Different Wetland and Non-wetland Classes

CLASS	LOWER SOUTH MCQUESTEN		SPRAGUE CREEK		MID SOUTH MCQUESTEN		HAGGARD CREEK		MAYO LAKE	
	KM²	%	KM²	%	KM²	%	KM²	%	KM²	%
Shallow water	0.04	0.01	0.06	0.01	1.10	0.26	0.05	0.01	0.40	0.10
Marsh	0.80	0.19	0.02	<0.01	0.911	0.22	0.05	0.01	2.14	0.51
Fen	2.47	0.59	2.02	0.48	28.19	6.70	9.60	2.28	28.02	6.66
Bog	0.00	0.00	0.34	0.08	0.09	0.02	0.30	0.07	2.45	0.58
Swamp	1.64	0.39	2.84	0.68	15.34	3.65	2.08	0.49	13.74	3.27
Deep water	2.21	0.53	0.63	0.15	2.25	0.54	0.52	0.12	102.74	24.44
Exposed disturbed	21.26	5.06	23.17	5.51	13.85	3.29	20.04	4.77	130.59	31.06
Forested/shrub	390.11	92.79	216.89	51.59	392.29	93.30	294.11	69.95	765.92	182.17
Grassland	1.91	0.45	0.00	0.00	0.00	0.00	0.00	0.00	0.00	0.00
Total (Wetland)	*4.95*	*1.18*	*5.28*	*2.15*	*45.63*	*10.05*	*12.08*	*3.70*	*46.75*	*4.50*
Total (Non-wetland)	*415.49*	*98.82*	*240.69*	*97.85*	*408.39*	*89.95*	*314.67*	*96.30*	*999.25*	*95.50*
Grand Total	**420.44**	**100.00**	**245.97**	**100.00**	**454.02**	**100.00**	**326.75**	**100.00**	**1,046.0**	**100.00**

4.3 CLASSIFICATION ASSESSMENT

The wetland classification was visually assessed by WSP, Government of Yukon, and First Nation of Na-Cho Nyak Dun and comments were incorporated in the final product. Based on review, most of the classified areas appeared to be visually realistic, conforming to landscape patterns, and corresponding with features visible in the Esri Basemap and SPOT 6/7 imagery. Focus was given to refining wetland polygons with the areas of special interest (Haggard Creek, Mayo Lake, Sprague Creek, and the Lower-South and Mid-South McQuesten), and as such some anomalous polygons may exist in other parts of the study area (e.g., shoreline swamps that cross over open water features).

Furthermore, the accuracy of the produced classification was statistically assessed using a confusion matrix obtained based on the classification, and combined field and interpreted sites set aside for product validation. Tables 11 and 12 provide the overall classification accuracy (OA), classification accuracy for each class (PA and UA) for the Mayo and McQuesten watersheds, and Table 13 provides the amount of misclassification (confusion) between various class pairs on a per pixel basis. The pixel-based accuracy assessment indicates the likelihood that a randomly selected pixel was classified correctly. Wetland extent across the Mayo and McQuesten watersheds was mapped with an accuracy of 98.66% (Kappa coefficient equals 0.98). The five major wetland classes were mapped with an accuracy of 88.32% (Kappa coefficient equals 0.82) within the study area. Of the wetland classes, shallow water obtained the highest PA (95.64%), indicating that most of the assessment data was correctly classified. The swamp class obtained a moderately high PA (72.28%), relative to the other vegetated wetland classes; however, the swamp class also had the lowest PA and UA, indicating that there were several field samples of other four wetland classes which were wrongly classified as swamp. As expected, the highest amount of confusion was between the fen and swamp or bog classes where swamp and bog assessment sites were incorrectly classified as fen. This confusion is likely due to the similarity between these classes which all have coniferous treed or shrubby forms overlaying organic soils (Environment Yukon 2019). Additionally, these three

wetland classes often transition between each other resulting in sites that have characteristics of multiple classes limiting the ability to separate these classes based solely on spectral signatures. Marsh was most often confused with shallow water. In Yukon, marshes are less common on the landscape in comparison to peatlands or swamps, and where they do occur, they tend to be limited to thin bands along shorelines. The 10 m spatial resolution Sentinel-2 imagery used in this project may not be able to properly capture these features, which could be addressed through the inclusion of high-resolution imagery such as SPOT. Although there was some confusion between some of the wetland classes, the accuracy levels that are obtained in this study for wetland classes are high considering the complexity of wetland landscapes in Yukon.

Table 11: The Overall, Producer, and User Classification Accuracies for Deep Water, Wetlands, and Uplands on a Per Pixel Basis for the Mayo and McQuesten Watersheds

OVERALL ACCURACY: 98.66%	KAPPA COEFFICIENT: 0.98	USER ACCURACY (%)
CLASS	PRODUCER ACCURACY (%)	
Deep Water	99.78	99.69
Wetland	98.09	93.14
Upland	97.71	99.48

Table 12: The Overall, Producer, and User Classification Accuracies of Wetland Classes on a Per Pixel Basis for the Mayo and McQuesten Watersheds

OVERALL ACCURACY: 88.32%	KAPPA COEFFICIENT: 0.82	USER ACCURACY (%)
CLASS	PRODUCER ACCURACY (%)	
Shallow water	95.64	92.57
Marsh	85.71	94.62
Fen	90.71	92.44
Bog	83.18	82.12
Swamp	72.28	71.86

Table 13: Confusion Matrix Obtained Based on the Produced Wetland Classification Calculated on a Per Pixel Basis for the Mayo and McQuesten Watersheds

MAPPED CLASS	REFERENCE SAMPLES (PERCENT OF PIXELS)					
		BOG	FEN	SWAMP	MARSH	SHALLOW WATER
	Non-wetland	0.77	1.11	11.68	3.68	0.08
	Bog	83.18	4.99	0.00	0.00	0.00
	Fen	15.96	90.71	16.04	5.28	0.00
	Swamp	0.08	2.51	72.28	0.43	0.40
	Marsh	0.00	0.67	0.00	85.71	3.88
	Shallow Water	0.00	0.00	0.00	4.90	95.64

An object-based accuracy assessment was additionally produced at the polygon level using the 50% of the manually delineated field and interpreted polygons set aside for assessment and is presented along with the class PA and UA in Appendix B. The object-based accuracy assessment indicates how likely a wetland or non-wetland polygon of interest was classified correctly. Based on the confusion matrix produced from the classified objects, an

OA of 80.87% was achieved when combing the wetland and non-wetland classes; however, the bog and swamps classes exhibited low PA and UA.

5 DISCUSSION

The results of this study show that regardless of the satellite data being used, wetlands due to their complexity, can hinder the achievement of higher classification accuracies compared to other land covers. For instance, wetland classes have several spectral similarities due to their biological and hydrological characteristics (Mitsch and Gosselink 2000; Amani et al. 2018a). Considering these facts and comparing the results with other wetland studies, the produced overall wetland classification accuracy of 88.32% in this project is very good. However, some confusion still existed between wetland classes most notably between fens, swamps, and bogs, as well as between marshes and shallow water (<2 m). In both cases this confusion is likely the result of overlapping ecosite characteristics, such as species and wetness. For example, wooded coniferous fens and swamps can host similar species and differ based on the specific characteristics of the soil and vegetation (i.e., size), which are not readily observed in satellite imagery. While the combination of optical, SAR, and topographical data improved the separability between similar classes, wetlands themselves are highly variable and transitional ecosystems making them difficult to classify both on the ground and through remote sensing methods.

As previously discussed, a supervised RF algorithm was used to classify wetlands within the study area. Within this framework, both the quality and the quantity of the field samples have a significant impact on the classification accuracy of a supervised classification. The field surveys completed as part of this project are in part to be used to develop an ecosite guide for the region. As such, the ecosite designations may change pending further examination, which would not be reflected in the data used to train the RF model. This may be the cause of some of the errors observed (e.g., a site initially called a fen is used to train the model but is a swamp). As well, grasslands were not well captured in the field data and it is difficult to determine if this is related to sampling design, lack of ecosite presence within the study area, or that grasslands occur in other areas of the region that were not the focus of the field campaign (e.g., alpine). Therefore, grasslands in the produced map were limited to the Lower South McQuesten area of special interest which was confirmed in the field to exhibit the grassland ecosite described in Environment Yukon (2019). Subsequent field data will be required to train the RF model on grasslands for the entirety of the Mayo and McQuesten watersheds, if desired. The field data was supplemented with satellite interpreted sites to increase the quantity of training data; however, there is some uncertainty inherent in the interpreted data as it relied on what was observable in the satellite imagery. In particular, water depth was difficult to determine from the imagery limiting the number of interpreted shallow water samples. As well, no shallow water sites were collected in the field, which additionally limited the training and assessment of the shallow water class. Wooded coniferous wetlands, a form of bogs, fens, and swamps, can also appear similar in satellite imagery, resulting in errors in the assigning of training data which would be propagated into the final classification. Increasing the quantity of training data assists in minimizing these errors, such that one erroneous site has less of an impact on the model but may still have impacted the classification accuracy as observed in Tables 11 to 13 (see also Appendix B).

Amani et al. (2020) found that the inclusion of high-resolution imagery improved the delineation of small landscape features, which was confirmed during preliminary tuning of the segmentation parameters. Government of Yukon has near full coverage of SPOT 6/7 imagery for the Mayo and McQuesten watersheds; however, this imagery was unable to be incorporated in the segmentation and classification due to technical and logistical limitations. For example, initial SPOT 6/7 imagery was noted to have incorrect georeferencing in certain scenes, as well as significant cloud cover in some areas, variable image date, and non-optimal timing (i.e., imagery not captured during peak growing season). Additional imagery was made available at a lower bit depth (8 bit as

opposed to 16 bit), though not all images possessed RGB or NIR bands. Due to the significant technical challenges in incorporating the SPOT 6/7 imagery and project timelines, it was decided to omit the imagery from segmentation and classification and reserve it for site interpretation and visual accuracy assessment of the final product. Government of Yukon intends to address the limitations with the SPOT imagery going forward.

6 CONCLUSION

WSP developed an object-based RF model that identified wetlands (i.e., shallow water, marsh, fen, bog, swamp) and non-wetlands (i.e., deep water, non-wetland, anthropogenic) within the Mayo and McQuesten watersheds. According to the results, about 7% of the total area within the study area comprises of wetlands while they cover only approximately 5% of the sub-basins. In comparison, Yukon Ecoregions Working Group (2004, p. 197-206) estimated that 5% of the Yukon Plateau North ecoregion, which the Mayo and McQuesten watersheds reside in, is covered in wetlands. The majority of wetlands occur within valley bottoms along notable watercourses, such as the McQuesten and Mayo Rivers. Large wetland complexes also occur along the Silver Trail. Of the wetland classes, fens were the most dominant by area. The overall wetland classification accuracy was 88.32%, with all producer's and user's accuracies of the wetland classes being >80% with the exception of swamp which was always >70%. These results show that the approach used in this project has a high potential for wetland classification in future studies and will assist in management decisions related to land use planning and management of the Mayo and McQuesten watersheds.

7 REFERENCES

Adam, E., O. Mutanga and D. Rugege. 2010. *Multispectral and Hyperspectral Remote Sensing for Identification and Mapping of Wetland Vegetation: A Review*. Wetlands Ecology and Management, 18(3), 281-296.

Adeli, S., B. Salehi, M. Mahdianpari, L.J. Quackenbush, B. Brisco, H. Tamiminia, and S. Shaw. 2020. *Wetland Monitoring using SAR Data: A Meta-analysis and Comprehensive Review*. Remote Sensing, 12(14), 2190.

Amani, M., B. Salehi, S. Mahdavi, and B. Brisco. 2018a. *Spectral Analysis of Wetlands using Multi-source Optical Satellite Imagery*. ISPRS journal of photogrammetry and remote sensing, 144, 119-136.

Amani, M., B. Salehi, S. Mahdavi, B. Brisco, and M. Shehata. 2018b. *A Multiple Classifier System to Improve Mapping Complex Land Covers: A Case Study of Wetland Classification using SAR Data in Newfoundland, Canada*. International Journal of Remote Sensing, 1-14.

Amani, M., B. Salehi, S. Mahdavi, and B. Brisco. 2019. *Separability Analysis of Wetlands in Canada using Multi-source SAR Data*. GIScience & Remote Sensing, 56(8), 1233-1260.

Amani, M., B. Salehi, S. Mahdavi, J. Granger, and B. Brisco. 2017a. *Wetland Classification in Newfoundland and Labrador using Multi-source SAR and Optical Data Integration*. GIScience & Remote Sensing, 54(6), 779-796.

Amani, M., B. Salehi, S. Mahdavi, J.E. Granger, B. Brisco, and A. Hanson. 2017b. *Wetland Classification using Multi-source and Multi-temporal Optical Remote Sensing Data in Newfoundland and Labrador, Canada*. Canadian Journal of Remote Sensing, 43(4), 360-373.

Amani, M., S. Mahdavi and O. Berard. 2020. *Supervised Wetland Classification using High Spatial Resolution Optical, SAR, and LiDAR Imagery*. Journal of Applied Remote Sensing, 14(2), 024502.

Baatz, M. 2000. *Multi Resolution Segmentation: An Optimum Approach for High Quality Multi Scale Image Segmentation*. In Beutragezum AGIT-Symposium. Salzburg, Heidelberg, 2000 (pp. 12-23).

Blaschke, T. 2010. *Object Based Image Analysis for Remote Sensing*. ISPRS journal of photogrammetry and remote sensing, 65(1), 2-16.

Breiman, L. 2001. *Random Forests*. Machine learning, 45(1), 5-32.

Cohen, J. 1960. *A Coefficient of Agreement for Nominal Scales*. Educational and Psychological Measurement, 20(1), 37-46.

Corcoran, J., J. Knight, K. Pelletier, L. Rampi, and Y. Wang. 2015. *The Effects of Point or Polygon-based Training Datamon Random Forest Classification Accuracy of Wetlands*. Remote Sensing, 7(4), 4002–4025.

CryoGeographic Consulting. 2018. *Mapping and Classifying Wetlands in the Indian River Alley, Yukon*. CryoGeographic Consulting and Palmer Environmental Consulting Group Inc., Whitehorse, YT, Canada.

Environment Yukon. 2016. *Yukon Ecological and Landscape Classification and Mapping Guidelines (Version 1.0).* Department of Environment, Government of Yukon, Whitehorse, YT, Canada.

Environment Yukon. 2019. *Klondike Plateau Boreal Low Subzone (BOLkp): A Field Guide to Ecosite Identification*. Department of Environment, Government of Yukon, Whitehorse, YT, Canada.

Gopal, S. and C. Woodcock. 1992. *Accuracy Assessment of the Stanislaus Vegetation Map using Fuzzy Sets*. Remote Sensing and Natural Resource Management: Proceedings of the Fourth Forest Service Remote Sensing Applications Conference, 378-394. American Society for Photogrammetry and Remote Sensing, USA.

Mahdavi, S., B. Salehi, J. Granger, M. Amani, B. Brisco, and W. Huang. 2018. *Remote Sensing for Wetland Classification: A Comprehensive Review*. GIScience & remote sensing, 55(5), 623-658.

Mahdavi, S., B. Salehi, M. Amani, J.E. Granger, B. Brisco, W. Huang, and A. Hanson. 2017. *Object-based Classification of Wetlands in Newfoundland and Labrador using Multi-temporal PolSAR Data*. Canadian Journal of Remote Sensing, 43(5), 432-450.

Mahdianpari, M., B. Brisco, J.E. Granger., F. Mohammadimanesh, B. Salehi, S. Homayouni, and L. Bourgeau-Chavez. 2021. *The Third Generation of Pan-Canadian Wetland Map at 10 m Resolution using Multisource Earth Observation Data on Cloud Computing Platform*. IEEE Journal of Selected Topics in Applied Earth Observations and Remote Sensing 14 (2021): 8789-8803.

Merchant, M.A., C. Hass, J. Schroder, R.K. Warren, and R. Edwards. 2020. *High-latitude Wetland Mapping using Multidate and Multisensor Earth Observation Data: A Case Study in the Northwest Territories*. Journal of Applied Remote Sensing 14, no. 3 (2020): 034511.

Merchant, M.A., R.K. Warren, R. Edwards, and J.K. Kenyon. 2019. *An Object-Based Assessment of Multi Wavelength SAR, Optical Imagery and Topographical Datasets for Operational Wetland Mapping in Boreal Yukon, Canada*. Canadian Journal of Remote Sensing.

Millard, K. and M. Richardson. 2013. *Wetland Mapping with LiDAR Derivatives*, SAR Polarimetric Decompositions, and LiDAR–SAR Fusion using a Random Forest Classifier Canadian Journal of Remote Sensing, 39(4), 290-307.

Mitsch, W.J. and J.G. Gosselink. 2000. *Wetlands*, third ed. Wiley, New York.

Moore, I.D., R.B. Grayson, and A.R. Ladson. 1991. *Digital Terrain Modelling: A Review of Hydrological, Geomorphological, and Biological Applications Hydrological Processes*, 5(1), 3-30.

National Wetlands Working Group. 1997. *The Canadian Wetland Classification System*. National Wetland Working Group, University of Waterloo, Wetlands Research Centre, Waterloo, ON, Canada.

Natural Resources Canada. 2013. *Canadian Digital Elevation Model: Product Specifications – Edition 1.1*. Government of Canada, Ottawa, ON, Canada.

Nobre, A.D., L.A. Cuartas, M. Hodnett, C.D. Rennó, G. Rodrigues, A. Silveira, and S. Saleska. 2011. *Height Above the Nearest Drainage–a hydrologically Relevant New Terrain Model*. Journal of Hydrology, 404(1-2), 13-29.

O'Neil, G.L., J.L. Goodall and L.T. Watson. 2018. *Evaluating the Potential for Site-specific Modification of LiDAR DEM Derivatives to Improve Environmental Planning-scale Wetland Identification using Random Forest Classification*. Journal of Hydrology, 559, 192-208.

Ozesmi, S.L. and M.E. Bauer. 2002. *Satellite Remote Sensing of Wetlands*. Wetlands Ecology and Management, 10(5), 381-402.

Porter, C., P. Morin, I. Howat, M-J Noh, B. Bates, K. Peterman, S. Keesey, M. Schlenk, J. Gardiner, K. Tomko, M. Willis, C. Kelleher, M. Cloutier, E. Husby, S. Foga, H. Nakamura, M. Platson, M. Wethington Jr,

C. Williamson, G. Bauer, J. Enos, G. Arnold, W. Kramer, P. Becker, A. Doshi, C. D'Souza, P. Cummens, F. Laurier, and M. Bojesen. 2018. ArcticDEM. [Data set]. Polar Geospatial Center and Harvard Dataverse.

Yukon Ecoregions Working Group. 2004. *Yukon Plateau-North*. In: Ecoregions of the Yukon Territory: Biophysical properties of Yukon landscapes, C.A.S. Smith, J.C. Meikle and C.F. Roots (eds.), Agriculture and Agri-Food Canada, PARC Technical Bulletin No. 04-01, Summerland, British Columbia, p. 63-72.

Appendix A

Imagery Data Sources

SENTINEL-2 IMAGES

Sentinel-2 Level 2A products are presented in granules, also called tiles, 110 km^2 by 110 km^2 ortho-images projected in WGS84 UTM. Each tile overlaps its neighbouring tiles considerably. The tile grid can be downloaded in KML format at:
https://sentinels.copernicus.eu/documents/247904/1955685/S2A_OPER_GIP_TILPAR_MPC__20151209T095117_V20150622T000000_21000101T000000_B00.kml

Table A1: List of Sentinel-2 Images used to Create the Median Mosaic for the Object-based Random Forest Classification

PLATFORM	SENSING DATE	TILE	ORBIT	CLOUDY PIXEL PERCENTAGE	CLOUD SHADOW PERCENTAGE	SNOW/ICE PERCENTAGE
Sentinel-2B	July 31, 2020	O7VFL	Ascending	0.29	0.05	0.00
Sentinel-2B	July 31, 2020	07WFM	Ascending	2.41	0.32	0.03
Sentinel-2B	July 31, 2020	08VLR	Ascending	0.48	0.05	0.00
Sentinel-2A	July 01, 2021	07VFL	Descending	1.08	0.74	0.00
Sentinel-2A	July 01, 2021	07WFM	Descending	0.69	0.70	0.26
Sentinel-2A	July 01, 2021	08VLR	Descending	0.98	0.69	0.00
Sentinel-2A	July 01, 2021	08VMR	Descending	2.23	1.49	0.09
Sentinel-2A	July 05, 2021	08VMR	Descending	4.45	0.96	0.00
Sentinel-2B	July 16, 2021	08VMR	Ascending	1.94	0.08	0.02
Sentinel-2B	July 16, 2021	08VNR	Ascending	0.22	0.12	0.00
Sentinel-2B	July 30, 2021	08VMR	Descending	0.00	0.00	0.00
Sentinel-2B	July 30, 2021	08VNR	Descending	4.33	3.89	0.02
Sentinel-2A	July 31, 2021	07VFL	Ascending	3.66	3.09	0.04
Sentinel-2A	July 31, 2021	08VLR	Ascending	3.76	3.15	0.04
Sentinel-2A	July 31, 2021	08VMR	Ascending	2.08	1.70	0.02
Sentinel-2A	July 31, 2021	08VNR	Ascending	0.42	0.62	0.00
Sentinel-2B	August 02, 2021	08WMS	Ascending	2.91	0.17	0.03
Sentinel-2A	August 31, 2021	08VMR	Ascending	2.22	2.40	0.00

SENTINEL-1 IMAGES

Sentinel-1 images were acquired as pre-processed Ground Range Detected, Interferometric Wide swath mode, Level 1 images in both VV and VH polarizations from Google Earth Engine. Interferometric Wide swath mode is the main acquisition mode over land and satisfies most project requirements, including wetland classification.

Table A2: List of Sentinel-1 Images used to Create the C-band SAR Mosaic for the Object-based Random Forest Classification

PLATFORM	SENSING DATE	ORBIT	IDENTIFIER
Sentinel-1A	July 01, 2020	Ascending	S1A_IW_GRDH_1SDV_20200701T022313_20200701T022338_033255_03DA55_D82A
Sentinel-1A	July 11, 2020	Ascending	S1A_IW_GRDH_1SDV_20200711T023944_20200711T024009_033401_03DEBA_6463
Sentinel-1A	July 13, 2020	Ascending	S1A_IW_GRDH_1SDV_20200713T022314_20200713T022339_033430_03DFA8_88B8
Sentinel-1A	July 23, 2020	Ascending	S1A_IW_GRDH_1SDV_20200723T023945_20200723T024010_033576_03E41D_1CCC
Sentinel-1A	July 25, 2020	Ascending	S1A_IW_GRDH_1SDV_20200725T022315_20200725T022340_033605_03E506_8FE2
Sentinel-1A	August 04, 2020	Ascending	S1A_IW_GRDH_1SDV_20200804T023946_20200804T024011_033751_03E972_1B9B
Sentinel-1A	August 06, 2020	Ascending	S1A_IW_GRDH_1SDV_20200806T022316_20200806T022341_033780_03EA71_7C69
Sentinel-1A	August 16, 2020	Ascending	S1A_IW_GRDH_1SDV_20200816T023946_20200816T024011_033926_03EF7D_EDA3
Sentinel-1A	August 18, 2020	Ascending	S1A_IW_GRDH_1SDV_20200818T022316_20200818T022341_033955_03F08E_5E37
Sentinel-1A	August 28, 2020	Ascending	S1A_IW_GRDH_1SDV_20200828T023947_20200828T024012_034101_03F5A5_9A5F
Sentinel-1A	August 30, 2020	Ascending	S1A_IW_GRDH_1SDV_20200830T022317_20200830T022342_034130_03F6BA_0F67

ALOS PALSAR IMAGES

ALOS PALSAR images were acquired as pre-processed Fine Bean Dual mode images in both HH and HV polarizations from the Alaska Satellite Facility (see https://asf.alaska.edu/).

Table A3: List of ALOS PALSAR Images used to Create the L-band SAR Mosaic for the Object-based Random Forest Classification

PLATFORM	SENSING DATE	ORBIT	GRANULE	PATH	FRAME
ALOS	August 27, 2010	Ascending	ALPSRP244511280	235	1280
ALOS	August 27, 2010	Ascending	ALPSRP244511270	235	1270
ALOS	August 22, 2010	Ascending	ALPSRP243781280	232	1280
ALOS	August 22, 2010	Ascending	ALPSRP243781270	232	1270
ALOS	August 15, 2010	Ascending	ALPSRP242761280	237	1280
ALOS	August 15, 2010	Ascending	ALPSRP242761270	237	1270
ALOS	August 02, 2009	Ascending	ALPSRP187621270	231	1270
ALOS	August 04, 2008	Ascending	ALPSRP134671280	234	1280
ALOS	August 04, 2008	Ascending	ALPSRP134671270	234	1270

Appendix B

Supplemental Assessments of Classification Accuracy

SUPPLEMENTAL PIXEL-BASED ASSESSMENTS

Table B1: The Overall, Producer, and User Accuracies of Wetland and Non-wetland Classes, Calculated Through a Pixel-based Assessment, within the Areas of Special Interest

OVERALL ACCURACY: 96.55%	KAPPA COEFFICIENT: 0.93	USER ACCURACY (%)
CLASS	PRODUCER ACCURACY (%)	
Wetland Class		
Shallow water	93.43	80.50
Marsh	88.26	96.83
Fen	96.83	86.29
Bog	89.46	86.71
Swamp	73.20	74.14
Non-wetlands		
Deep water	96.68	93.84
Exposed/disturbed	99.68	96.05
Forested/shrub	97.09	99.29
Grassland	84.19	100.00

Table B2: Confusion Matrix Obtained Based on the Produced Classification Calculated on a Per Pixel Basis for the Entire Mayo and McQuesten Watersheds

MAPPED CLASS	REFERENCE SAMPLES (PERCENT OF PIXELS)								
	DEEP WATER	SHALLOW WATER	MARSH	FEN	BOG	SWAMP	EXPOSED/ DISTURBED	FORESTED/ SHRUB	GRASSLAND
Deep water	99.78	0.00	3.37	0	0	0.00	0.00	0.18	0
Shallow water	0.04	95.64	4.90	0	0	0.00	0.10	0.00	0
Marsh	0.10	3.88	85.71	0.67	0	0.00	0.00	0.00	0
Fen	0.01	0.00	5.28	90.71	15.94	16.04	0.00	1.71	0
Bog	0.00	0.00	0.00	4.99	83.2	0.00	0.00	0.41	0
Swamp	0.01	0.40	0.43	2.51	0.08	72.28	0.00	0.44	0
Exposed/ Disturbed	0.01	0.00	0.00	0.51	0	0.00	97.61	0.44	12.11
Forested/ Shrub	0.06	0.08	0.31	1.11	0.78	11.68	2.29	96.81	3.7
Grassland	0.00	0.00	0.00	0	0	0.00	0.00	0.00	84.19

Table B3: Confusion Matrix Obtained Based on the Produced Classification Calculated on a Per Pixel Basis for the Areas of Special Interest

MAPPED CLASS	REFERENCE SAMPLES (PERCENT OF PIXELS)								
		DEEP WATER	SHALLOW WATER	MARSH	FEN	BOG	SWAMP	EXPOSED/ DISTURBED	FORESTED/ SHRUB	GRASSLAND
	Deep water	96.68	0.00	5.01	0	0	0.00	0.00	0.00	0
	Shallow water	0.00	93.43	1.18	0	0	0.00	0.00	0.00	0
	Marsh	0.00	0.00	88.26	0.84	0	0.00	0.00	0.00	0
	Fen	0.48	0.00	4.75	96.83	9.95	12.50	0.00	1.84	0
	Bog	0.00	0.00	0.00	0.37	89.46	0.00	0.00	0.24	0
	Swamp	0.29	6.57	0.65	0.37	0	73.20	0.00	0.32	0
	Exposed/ Disturbed	0.34	0.00	0.00	0	0	0.00	99.68	0.54	12.11
	Forested/ Shrub	2.21	0.00	0.15	1.6	0.59	14.30	0.32	97.07	3.7
	Grassland	0.00	0.00	0.00	0	0	0.00	0.00	0.00	84.19

SUPPLEMENTAL OBJECT-BASED ASSESSMENTS

Table B4: The Overall, Producer, and User Accuracies of Wetland and Non-wetland Classes, Calculated Through an Object-based Assessment

OVERALL ACCURACY: 80.87%	KAPPA COEFFICIENT: 0.76	USER ACCURACY (%)
CLASS	PRODUCER ACCURACY (%)	
Wetland Class		
Shallow water	70.75	64.38
Marsh	64.80	78.64
Fen	72.60	63.22
Bog	45.83	63.77
Swamp	48.48	36.78
Non-wetlands		
Deep water	87.90	97.18
Exposed/disturbed	96.12	96.43
Forested/shrub	89.07	88.63
Grassland	50.00	100.00

Table B5: Confusion Matrix for Weltnad and Non-Wetland Classes Calculated on a Per Object Basis

MAPPED CLASS	REFERENCE SAMPLES (PIXELS)								
		DEEP WATER	SHALLOW WATER	MARSH	FEN	BOG	SWAMP	EXPOSED/ DISTURBED	FORESTED/ SHRUB	GRASSLAND
	Deep water	138	0	0	0	0	0	0	2	5
	Shallow water	8	47	17	0	0	0	1	0	0
	Marsh	5	11	81	6	0	0	0	0	0
	Fen	2	1	12	196	44	18	0	37	0
	Bog	0	0	0	22	44	0	0	3	0
	Swamp	3	5	3	22	3	32	0	19	0
	Exposed/ Disturbed	1	0	0	0	0	0	297	5	0
	Forested/ Shrub	0	3	10	24	5	16	11	538	0
	Grassland	0	0	0	0	0	0	0	0	5